Linc-ROR Modulates the Endothelial-Mesenchymal Transition of Endothelial Progenitor Cells through the miR-145/Smad3 Signaling Pathway

Jinqing LIANG[1#], Hairong CHU[1#], Yutong RAN[1#], Runling LIN[1], Yanbing CAI[1], Xiumei GUAN[1], Xiaodong CUI[1], Xiaoyun ZHANG[1], Hong LI[1], Min CHENG

[#]*These authors contributed equally to this work*

[1]School of Basic Medical Sciences, Shandong Second Medical University, Weifang, Shandong, China

Received December 14, 2023
Accepted March 12, 2024

Summary

The endothelial-mesenchymal transition (EndMT) of endothelial progenitor cells (EPCs) plays a notable role in pathological vascular remodeling. Emerging evidence indicated that long non-coding RNA-regulator of reprogramming (linc-ROR) can promote epithelial-mesenchymal transition (EMT) in a variety of cancer cells. Nevertheless, the function of linc-ROR in EPC EndMT has not been well elucidated. The present study investigated the effect and possible mechanisms of function of linc-ROR on the EndMT of EPCs. A linc-ROR overexpression lentiviral vector (LV-linc-ROR) or a linc-ROR short hairpin RNA lentiviral vector (LV-shlinc-ROR) was used to up or downregulate linc-ROR expression in EPCs isolated from human umbilical cord blood. Functional experiments demonstrated that LV-linc-ROR promoted the proliferation and migration of EPCs, but inhibited EPC angiogenesis *in vitro*. In the meantime, reverse transcription-quantitative PCR and western blotting results showed that the expression of the endothelial cell markers vascular endothelial-cadherin and CD31 was decreased, while the expression of the mesenchymal cell markers α-smooth muscle actin and SM22α was increased at both mRNA and protein levels in LV-linc-ROR-treated EPCs, indicating that linc-ROR induced EPC EndMT. Mechanistically, the dual-luciferase reporter assay demonstrated that microRNA (miR/miRNA)-145 was a direct target of linc-ROR, and miR-145 binds to the 3′-untranslated region of Smad3. Moreover, LV-shlinc-ROR increased the expression of miR-145, but decreased the expression of Smad3. In conclusion, linc-ROR promotes EPC EndMT, which may be associated with the miR-145/Smad3 signaling pathway.

Keywords

Endothelial progenitor cells • Endothelial to mesenchymal transition • Linc-ROR • MiR-145 • Atherosclerosis

Corresponding author

Hong Li, School of Basic Medical Sciences, Shandong Second Medical University, 7166 Baotongxi Road, Weicheng, Weifang, Shandong, P.R. China. E-mail: lh@sdsmu.edu.cn; Min Cheng, School of Basic Medical Sciences, Shandong Second Medical University, 7166 Baotongxi Road, Weicheng, Weifang, Shandong, P.R. China. E-mail: mincheng@sdsmu.edu.cn

Introduction

Endothelial injury is regarded as a crucial pathophysiological cause of cardiovascular diseases such as atherosclerosis [1]. It has been widely reported that endothelial progenitor cells (EPCs) from the bone marrow can migrate and differentiate into endothelial cells (ECs) to repair vascular injury [2,3]. However, accumulating evidence suggests that EPCs undergo endothelial-mesenchymal transition (EndMT), which may aggravate intimal hyperplasia and contribute to atherogenesis [4-6]. During this transition, the expression of endothelial-specific markers such as CD31 and vascular endothelial (VE)-cadherin is decreased, while that of mesenchymal-specific markers such as α-smooth muscle actin (α-SMA), and SM22 is increased. This transition promotes the proliferation and migration of EPCs, but inhibited angiogenesis. In the present study, a complex signaling network is proposed to be responsible for EPC EndMT.

Long non-coding RNAs (lncRNAs) contain >200 nucleotides with either little or non-protein-coding capacity. Increasing evidence indicated that lncRNAs

exert their functions by chromatin modification, and either transcriptional or post-transcriptional regulation [7,8]. LncRNAs play a marked role in the development of numerous diseases, such as tumors, diabetes, cardiovascular diseases, and so on. Although many lncRNAs can affect the EndMT process, the lncRNA-regulator of reprogramming (linc-ROR) has its own unique characteristics compared with previously reported factors. Linc-ROR was first discovered in induced pluripotent stem cells, maintains the reprogramming and self-renewal ability of cells by preventing the activation of cellular stress pathways, including the p53 response [9,10]. Moreover, subsequent studies have demonstrated that linc-ROR may function as a molecular sponge for microRNA (miR/miRNA)-145 to promote epithelial-mesenchymal transition (EMT) in a variety of cancer cells, such as nasopharyngeal, gallbladder, colorectal and gastric cancer cells [11,12]. Therefore, linc-ROR exhibited different regulatory functions in different cells. As a special form of EMT, EndMT shares a number of molecular mechanisms with EMT [13]. The role of linc-ROR in EPC EndMT remains unknown.

Previous studies have identified the Smad3 signaling pathway being involved in EndMT. Qiu *et al* [14] showed that Smad can bind to a Smad-binding element in the first exon of SM22α, and regulate the SM22α promoter through CArG box-dependent transcription. Moreover, Smad3 was required when TGF-β induced the synthesis of α-SMA [15]. Li *et al* [16] reported that inhibition of Smad3 with the inhibitor SIS3 restrained EndMT and delayed the progression of diabetic nephropathy. In the meantime, blockage of EndMT in human umbilical vein endothelial (HUVEC)-12 cells was associated with the suppression of the Smad signaling pathway [17]. As a precursor of ECs, Smad3 may also play a critical role in the EPC EndMT process.

The aim of the present study was to investigate the effect of linc-ROR on the EndMT of EPCs derived from human umbilical cord blood and the possible mechanisms.

Methods

EPC culture

A total of 20 ml fresh human umbilical cord blood was obtained from the Affiliated Hospital of Weifang Medical College. The experiments were in accordance with the Declaration of Helsinki (2000) of the World Medical Association and approved by the Ethics Committee of Weifang Medical University (approval no. WFMU-2018-288). Then, EPCs were cultured as previously described [18]. Briefly, total mononuclear cells (MNCs) were isolated by lymphocyte separation medium 1077 (cat. no. LTS1077; TBD; Tianjin Haoyang Biological Products Technology Co., Ltd.). Mononuclear cells were then inoculated in a cell flask precoated with 50 μg/ml human plasma fibronectin (cat. no. F0895; Sigma-Aldrich; Merck KGaA), and maintained in complete Endothelial Growth Medium-2 MV Bulletkit (EGM-2; cat. co. CC-3202; Lonza Group, Ltd.) containing 10 % fetal bovine serum at 37ºC in a 5 % CO_2 incubator. Culture medium was refreshed after 4 days to eliminate non-adherent cells. To determine the endothelial phenotype of EPCs, culture cells were characterized by the stain of DiL-Ac-LDL (cat. no. L3484; Invitrogen; Thermo Fisher Scientific, Inc.) and FITC-UEA-1 (cat. no. L32476; Invitrogen; Thermo Fisher Scientific, Inc.) under a fluorescence microscope. Generally, cells at passages 3-6, namely late EPCs, incubated for around 12-20 days, were used in subsequent experiments. Those cells express a variety of endothelial markers and functionally differentiate into mature ECs, promoting vascular integrity and neovascularization.

Lentiviral transfection

Cells were plated at a density of $1x10^6$ cells/well in a 6-well plate. When cells reached ~50 % confluence after 24 h, EPCs were transfected with linc-ROR overexpression lentiviral vector (LV-linc-ROR, GV367: Ubi-MCS-SV40-EGFP-IRES-puromycin, Shanghai GeneChem Co., Ltd.) to up linc-ROR expression compared with empty vector (LV-control). Similarly, linc-ROR short hairpin RNA lentiviral vector (LV-shlinc-ROR, GV493: hU6-MCS-CBh-gcGFP-IRES-puromycin, Shanghai GeneChem Co., Ltd.) targeting GCCTGAGAGTTGGCATGAA was synthesized to downregulate linc-ROR expression compared with control lentivirus with a scramble sequence: TTCTCCGAACGTGTCACGT (LV-scramble). The medium was replaced after 12 h, and the transfection efficiency was assessed by fluorescence intensity using a fluorescence microscope. Transfected cells were screened with puromycin 48 h later, and the overexpression or interference efficiency was confirmed by reverse transcription-quantitative PCR and the experiments were performed 72 h later.

Table 1. Primers used in qRT-PCR analysis.

Gene name		Primer sequences (5′—3′)
GAPDH	Forward	GCACCGTCAAGGCTGAGAAC
	Reverse	TGGTGAAGACGCCAGTGGA
linc-ROR	Forward	ATCGCCACTCTGCTTAGAACCT
	Reverse	CAGCCCTTTCCTCCTTGTTG
CD31	Forward	CCGCATATCCAAGGTCAGCA
	Reverse	CACCTTGGTCCAGATGTGTGAA
VE-cadherin	Forward	TGGCCTGTGTTCACGCATC
	Reverse	TCGTCTGCATCCACTGCTGTC
SM22α	Forward	ATGATGGGCACTACCGTGGA
	Reverse	CCCATCTGAAGGCCAATGAC
α-SMA	Forward	ATTGCCGACCGAATGCAGA
	Reverse	ATGGAGCCACCGATCCAGAC
miR-145	Forward	CAGTTTTCCCAGGAATCCCTA
	Reverse	Not disclosed by the company
U6	Forward	GGAACGATACAGAGAAGATTAGC
	Reverse	TGGAACGCTTCACGAATTTGCG

RT-qPCR

Total RNA was extracted using TRIzol™ reagent (cat. no. 15596018; Invitrogen; Thermo Fisher Scientific, Inc.), and reversely transcribed into cDNA using Evo M-MLVRT Master Mix (Hunan Accurate Bio-Medical Co., Ltd.) according to the manufacturer's instructions. SYBR Green Pro Taq HS Premix (Hunan Accurate Bio-Medical Co., Ltd.) was performed to amplify corresponding genes with an ABI StepOnePlus detection system according to the manufacturer's protocol. Primers of linc-ROR, CD31, vascular endothelial (VE)-cadherin, SM22α, α-SMA, miR-145, U6 and GAPDH were synthesized by Hunan Accurate Bio-Medical Co., Ltd., and the sequences are shown in Table 1. qPCR was carried out under the following conditions: 95 ºC for 30 sec; 40 cycles of 95 ºC for 5 sec and 60 ºC for 30 sec. GAPDH was used as an internal control. For miR-145, U6 was used as a normalization control. The relative expression changes were calculated using the $2^{-\Delta\Delta Cq}$ method.

Western blotting

EPC lysates were collected using RIPA lysis buffer (Beijing Solarbio Science & Technology Co., Ltd.). The BCA protein assay kit (cat. no. P0010; Beyotime Institute of Biotechnology) was used to detect protein concentrations. Proteins (8 μg/lane) were subjected to 12 % SDS-polyacrylamide gel electrophoresis, and then transferred to PVDF membranes (cat. no. HATF09025; Millipore). After blocking the membranes with 5 % skimmed milk in TBST (0.05 % Tween 20) for 60 min at room temperature, the membranes were incubated with anti-β-actin (1:2,000; cat. no. GB11001; Wuhan Servicebio Technology Co., Ltd.), anti-CD31 (1:1,000; cat. no. ab76533; Abcam), anti-VE-cadherin (1:1,000; cat. no. ab33168; Abcam), anti-Smad3 (1:1,000; cat. no. 9523; Cell Signaling Technology, Inc.), anti-SM22α (1:2,000; cat. no. ab14106; Abcam) and anti-α-SMA (1:1,000; cat. no. 19245; Cell Signaling Technology, Inc.) antibodies at 4 ºC overnight for 12-16 h. Next, the membranes were incubated with horseradish peroxidase (HRP)-conjugated secondary antibody at room temperature for 1 h. Membranes were visualized using Amersham Image Quant 800 after being coated with Omni-ECL™ luminous solution.

Cell proliferation assay

EPC proliferation was determined using the Cell Counting Kit-8 assay (cat. no. K1018; APeXBIO Technology LLC) and the 5-ethynyl-2'-deoxyuridine (EdU; cat. no. C10310-1; Guangzhou RiboBio Co., Ltd.) assay. For the CCK-8 assay, cells were plated at a density of 8,000 cells per well in a 96-well plate. After 24 h,10 μl CCK-8 solution and 100 μl medium were added, and cells were incubated at 37 ºC for 2 h. The optical density of 450 nm was detected using a microplate reader.

For the EdU assay, 0.1 µl EdU solution and 100 µl medium was added to the cells which were then incubated at 37 ºC for 2 h. Cells were fixed using 4 % paraformaldehyde (Beijing Solarbio Science & Technology Co., Ltd.) for 30 min at room temperature, and infiltrated with PBS containing 0.5 % Triton X-100 (Beijing Solarbio Science & Technology Co., Ltd.) for 10 min. Furthermore, Apollo® staining solution was used to measure cell proliferation at room temperature for 30 min, and Hoechst33342 solution (cat. no. 62249; Thermo Fisher Scientific, Inc.) was used to stain cell nuclei at room temperature for 15 min. Finally, stained cells were counted using a fluorescence microscope. Image-Pro Plus (version 6.0; Media Cybernetics, Inc.) was used to analyze the images.

Cell migration assay

Migration of EPCs was detected using a modified Boyden chamber assay. Briefly, the lower chamber was filled with 10 % EGM-2 medium, and 200 µl cell suspension containing 8,000 cells was added to the upper chamber. After a 10-h incubation, non-migrating cells in the upper chamber were removed with cotton swabs. Subsequently, EPCs were fixed with 4 % paraformaldehyde at room temperature for 30 min, and cell nuclei were stained with DAPI (Beijing Solarbio Science & Technology Co., Ltd.) at room temperature for 15 min. The average number of migratory cells was viewed and counted under a fluorescence microscope.

Tube formation assay in vitro

A 96-well plate was coated with 75 µl Matrigel (cat. no. 356234; Corning, Inc.) at 37 ºC for 2 h. Subsequently, $2x10^4$ cells were seeded into every well and incubated for 10 h. Tube-like structure was detected using an inverted phase-contrast microscope. The length of complete tubes formed/unit area in every image was quantified and assessed using ImageJ (version 1.8.0; National Institutes of Health).

Dual-luciferase reporter assay

TargetScan Human (www.targetscan.org) was employed to predict the potential binding sites between linc-ROR/miR-145 and Smad3/miR-145. The recombinant plasmids pmirGLO-linc-ROR (Hunan Accurate Bio-Medical Co., Ltd.) containing miR-145 binding sites or pmirGLO-Smad3 (Hunan Accurate Bio-Medical Co., Ltd.) containing 3'untranslated region (UTR) were constructed, and Lipofectamine®3000 (cat. no. L3000015; Invitrogen; Thermo Fisher Scientific, Inc.) was used to co-transfect 293T cells with either miR-145 mimics (sense: 5′-GUCCAGUUUUCCCAGGAAU CCCU-3′, anisense: 5′-GGAUUCCUGGGAAAACU GG ACUU-3′) or miR-145 negative control (NC, sense: 5′-UUCUCCGAACGUGUCACGUTT-3′, anisense: 5′-ACGUGACACGUUCGGAGAATT-3′) respectively. After 48 h, the fluorescence of Firefly luciferase and Renilla luciferase were detected using the Dual-luciferase Reporter Assay System (cat. no. E1910; Promega Corporation) following the manufacturer's instructions. The relative luciferase activity was normalized to the activity of Renilla luciferase.

Statistical analysis

All experiments were repeated three times. All data were statistically analyzed, and presented as mean ± standard deviation. The Student's t-test was used to compared two groups. $P<0.05$ was considered to indicate a statistically significant significance.

Results

EPCs were cultured from umbilical cord blood

EPCs are heterogeneous, and can be classified as early and late EPCs. The early EPCs appear within 4-7 days, which have the properties of progenitor cells and can form colonies. While the late EPCs develop after 2-3 weeks in *ex vivo* culture systems, the passaged cells begin to differentiate into ECs and present with typical cobblestone-like morphology of mature ECs after ~12 days [19]. Although all EPC populations have been shown to contribute to angiogenesis, only late EPCs, have been demonstrated to possess the ability to form *de novo* blood vessels or become a part of the circulation system *in vivo* [20]. As shown in Fig. 1, MNCs derived from human umbilical cord blood showed distinct colonies 7 days later, and the cells demonstrated typical cobblestone-like morphology after 2 passages (Fig. 1A). Moreover, cells were positively staining for Dil-Ac-LDL (red) and FITC-UEA-1 (green; Fig. 1B).

After transfected with LV-linc-ROR or LV-shlinc-ROR 72 h later, the expression level of linc-ROR in the transfected cells was measured by RT-qPCR. The results showed that linc-ROR was successfully overexpressed or silenced after transfection with either LV-linc-ROR or LV-shlinc-ROR compared with the LV-control or LV-scramble group (Fig. 1C).

Linc-ROR promoted the migration and inhibited the angiogenesis of EPCs

The modified Boyden chamber assay was used to determine the effect of linc-ROR on the migration of EPCs. The results demonstrated that LV-linc-ROR markedly inhibited the migration of EPCs. Inversely, LV-shlinc-ROR increased EPC migration ability (Fig. 2A).

The Matrigel assay was used to study the effect of linc-ROR on the angiogenesis of EPCs *in vitro*. As shown in Fig. 2B, LV-linc-ROR inhibited the angiogenesis of EPCs. By contrast, LV-shlinc-ROR facilitated the angiogenesis of EPCs. These findings indicated that linc-ROR inhibited the angiogenesis of EPCs.

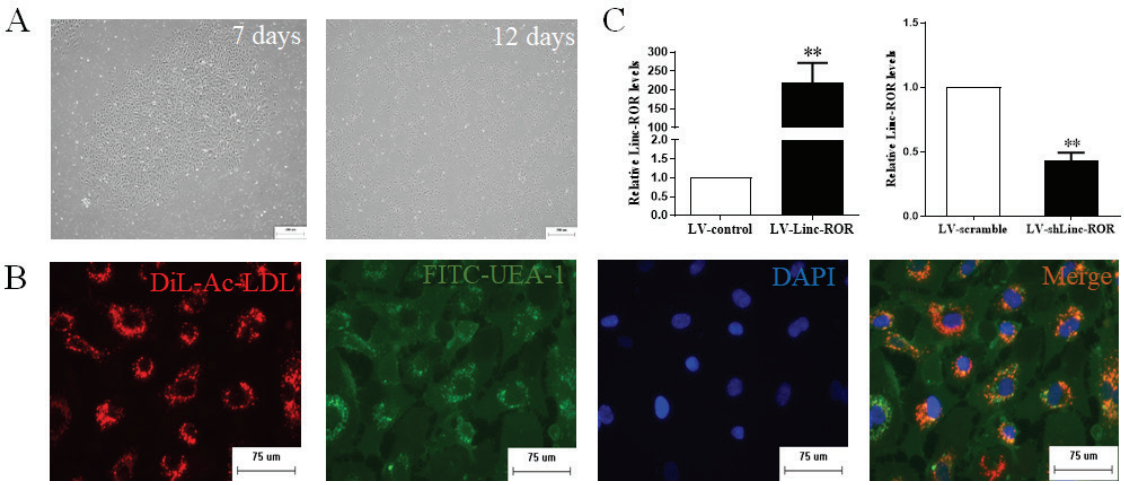

Fig. 1. EPCs were cultures from umbilical cord blood. (**A**) The isolated MNCs formed colonies approximately 7 days later. The passaged cells presented typical cobblestone-like morphology of ECs. Scale bar: 200 μm. (**B**) Most of the EPCs were double-stained with DiL-Ac-LDL (red fluorescence) and FITC-UEA-1 (green fluorescence) under a fluorescence microscope. Scale bar: 75 μm. (**C**) Linc-ROR was successfully overexpressed or silenced after transfection of LV-linc-ROR or LV-shlinc-ROR, respectively. n=3, ***P*<0.01 *vs.* the LV-control or LV-scramble group.

Linc-ROR promoted the proliferation of EPCs

The CCK-8 and EdU assays were used to determine the effect of linc-ROR on the proliferation of EPCs. The CCK-8 assay results showed that LV-linc-ROR significantly promoted cell proliferation, while LV-shlinc-ROR inhibited cell proliferation (Fig. 3A). Similarly, EdU assays confirmed that LV-linc-ROR increased the proliferation ability of EPCs. Conversely, LV-shlinc-ROR markedly inhibited the proliferation rate of EPCs (Fig. 3B).

Linc-ROR promoted the EndMT of EPCs

RT-qPCR and western blotting were undertaken to explore the effects of linc-ROR on the EndMT of EPCs. As shown in Fig. 4A and 4B, LV-linc-ROR decreased the expression of the endothelial markers CD31 and VE-cadherin at both mRNA and protein levels. However, the expression of the mesenchymal markers SM22α and α SMA, was promoted by LV-linc-ROR (Fig. 4C, D). By contrast, LV-shlinc-ROR showed the opposite results; LV-shlinc-ROR increased the expression of CD31 and VE-cadherin (Fig. 4E, F), but decreased the expression of SM22α and α-SMA at both mRNA and protein levels (Fig. 4G, H).

The miR-145/smad3 signaling pathway was involved in the EPC EndMT promoted by linc-ROR

Emerging evidence has shown the possible mechanism used by lncRNAs to inhibit the expression of target genes by sponging miRNAs. Therefore, TargetScan Human (http://www.targetscan.org) and miRanda databases (http://www.microrna.org/microrna/home.do) were employed to predict the potential binding sites between miRNAs and linc-ROR. The website prediction results showed that both of 3' untranslated region of the linc-ROR mRNA and Smad3 mRNA have the binding sites with miR-145 (Fig. 5A).

MiR-145 mimics could increase the miR-145 level in 293T cells compared with the NC group. The dual-luciferase reporter assay also showed that transfection of miR-145 mimics significantly inhibited the luciferase activity in 293T cells transfected with either pmirGLO-linc-ROR or pmirGLO-Smad3, while no

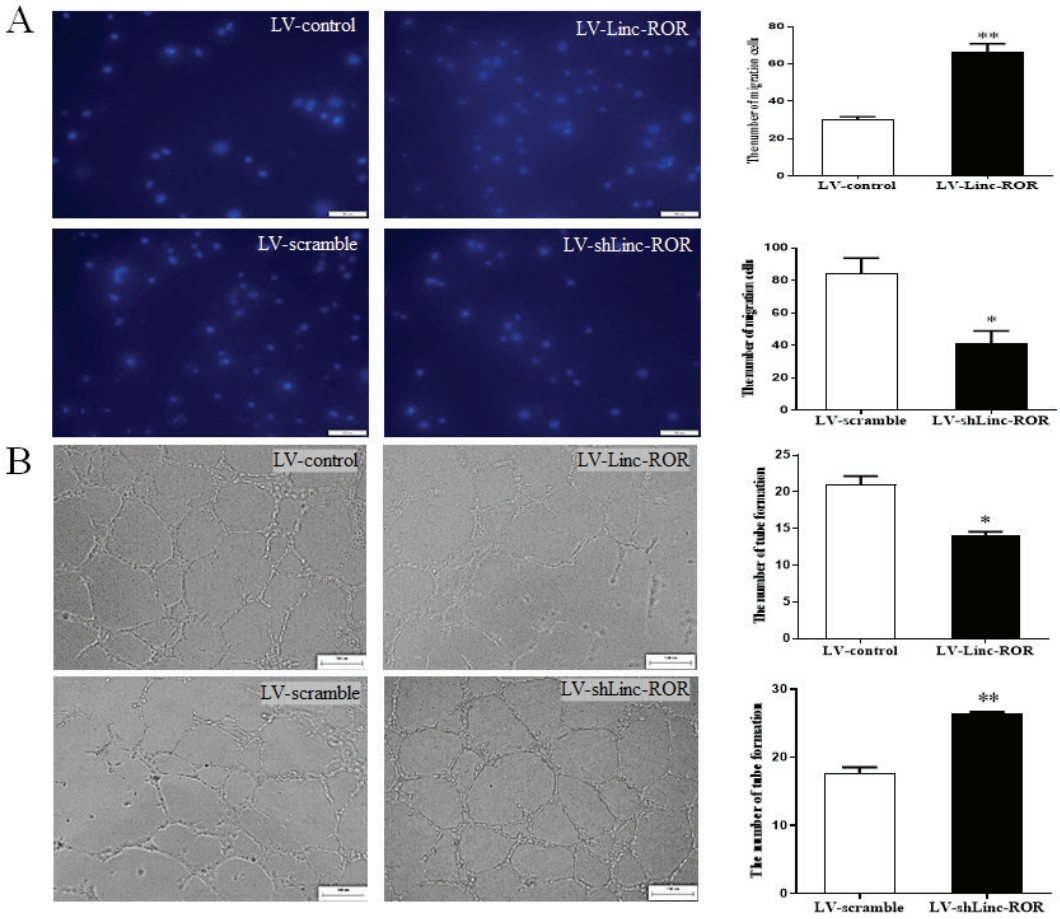

Fig. 2. Linc-ROR promoted the migration and inhibited the angiogenesis of EPCs. (**A**) The modified Boyden chamber result demonstrated that LV-linc-ROR promoted the migration of EPCs, but LV-shlinc-ROR inhibited the migration of EPCs. Scale bar: 50 μm. (**B**) The Matrigel result indicated that LV-linc-ROR significantly inhibited the angiogenesis of EPCs, but LV-shlinc-ROR increased the angiogenesis of EPCs *in vitro*. Scale bar: 100 μm. n=3, *P<0.05, **P<0.01 *vs.* the LV-control or LV-scramble group.

change of luciferase activities was found in miR-145 NC (Fig. 5B). These data suggested that linc-ROR effectively binds to miR-145, and miR-145 binds to the 3'UTR of Smad3 mRNA. In addition, RT-qPCR results demonstrated that LV-linc-ROR inhibited the expression of miR-145, while LV-shlinc-ROR increased the miR-145 levels in EPCs (Fig. 5C). Moreover, western blotting revealed that LV-linc-ROR promoted the protein expression of Smad3, but LV-shlinc-ROR inhibited the protein levels of Smad3 (Fig. 5D).

Discussion

Pathological vascular remodeling induced by the imbalance between endothelial cell damage and repair is a major pathophysiological feature of atherosclerosis [21]. However, the underlying mechanisms have not been fully elucidated.

EndMT plays an important role in the development of various tissues and organs, such as heart valve and septum formation during the embryonic stage. EndMT was also involved in the pathogenesis of multiple diseases, including pulmonary hypertension, atherosclerosis, cerebrovascular malformations, tissue fibrosis and cancer [22]. Increasing evidence has reported that EndMT is involved in the process of pathological vascular remodeling [23]. The physical and chemical factors that cause EndMT include hyperglycemia, hypoxia, oxidative stress, pro-inflammatory cytokines, oscillatory shear stress, endothelin-1, angiotensin II and others. Previous studies, including the present one, showed that EPCs transdifferentiated into mesenchymal cells may contribute to intimal hyperplasia and atherogenesis, and aggravate pathological vascular remodeling [18,24].

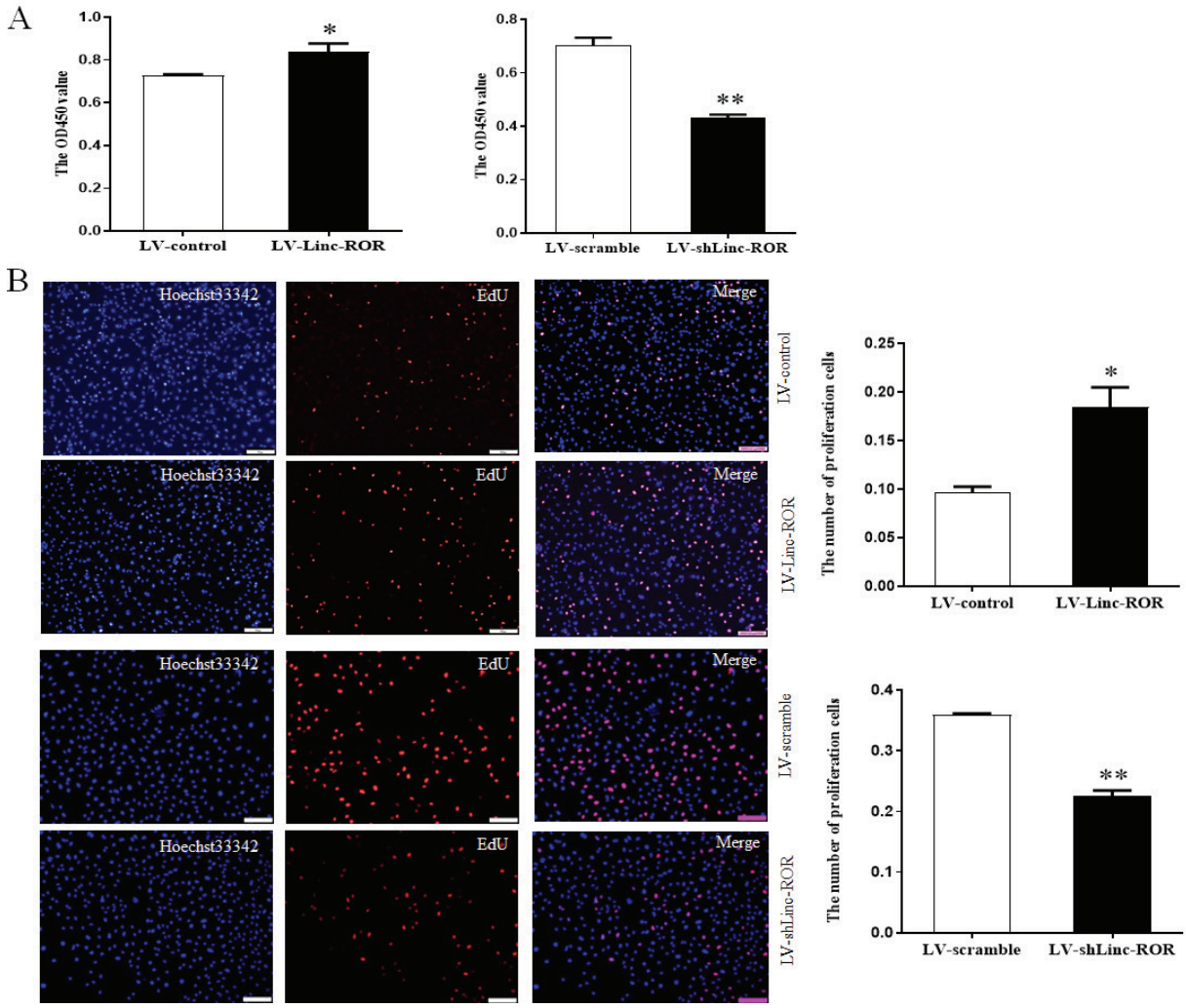

Fig. 3. Linc-ROR promoted the proliferation of EPCs. (**A**) The CCK-8 results showed that LV-linc-ROR obviously increased the proliferation of EPCs, but LV-shlinc-ROR inhibited the proliferation of EPCs. (**B**) The EdU results were consistent with the CCK-8 results. Red: EdU-stained positive cells, and blue: Hoechst33342-stained nuclei. Scale bar: 100 μm. n=3, **P*<0.05, ***P*<0.01 *vs.* the LV-control or LV-scramble group.

In recent years, accumulating evidence illustrated that lncRNAs play critical roles in EndMT. For example, lncRNA-GM16410 was involved in regulating PM2.5-induced pulmonary EndMT [25]. LncRNA ZFAS1 increased Notch3 expression and promoted ox-LDL-induced EndMT in HUVECs [26]. Similarly, Zhang *et al* [27] found that lncRNA TUG1 could regulate autophagy-mediated EndMT in hepatic sinusoidal cells. In the present study, it was shown that linc-ROR manifested a migratory and proliferative phenotype of EPCs, but inhibited EPC angiogenesis. In the meantime, EPCs decrease the expression of the endothelial cell specific markers VE-cadherin and CD31, and increase the expression of the mesenchymal cell markers α-SMA and SM22α. This suggests that linc-ROR is involved in EPC EndMT.

Linc-ROR is located in chromosome 18q21.31, spanning 2.6 kb and consisting of four exons [9]. Emerging evidence suggests that linc-ROR exerts pivotal roles in most types of human disorders, such as cancer, autoimmune disorders and neurodegenerative/ neuro-developmental disorders [28]. It can exert its role by affecting the activity of some signaling pathways and acting as a molecular sponge for some miRNAs, including miR-212-3p, miR-138, miR-145, miR-93-5p, miR320a, miR-320b and miR-876-5p [28,29]. For instance, linc-ROR regulated EMT, cellular proliferation and invasion of endometriosis through binding to miR-204-5p [10]. Moreover, linc-ROR was previously reported to alleviate hypoxia-induced damage by downregulating miR-145-5p in H9c2 cells [30]. Another study reported that linc-ROR mitigates cobalt

chloride-induced hypoxia injury through regulation of miR-145 [31]. In the present study, it was confirmed that linc-ROR has the binding sites with miR-145 using the dual-luciferase assay. In addition, RT-qPCR results showed that LV-linc-ROR inhibited the expression of miR-145.

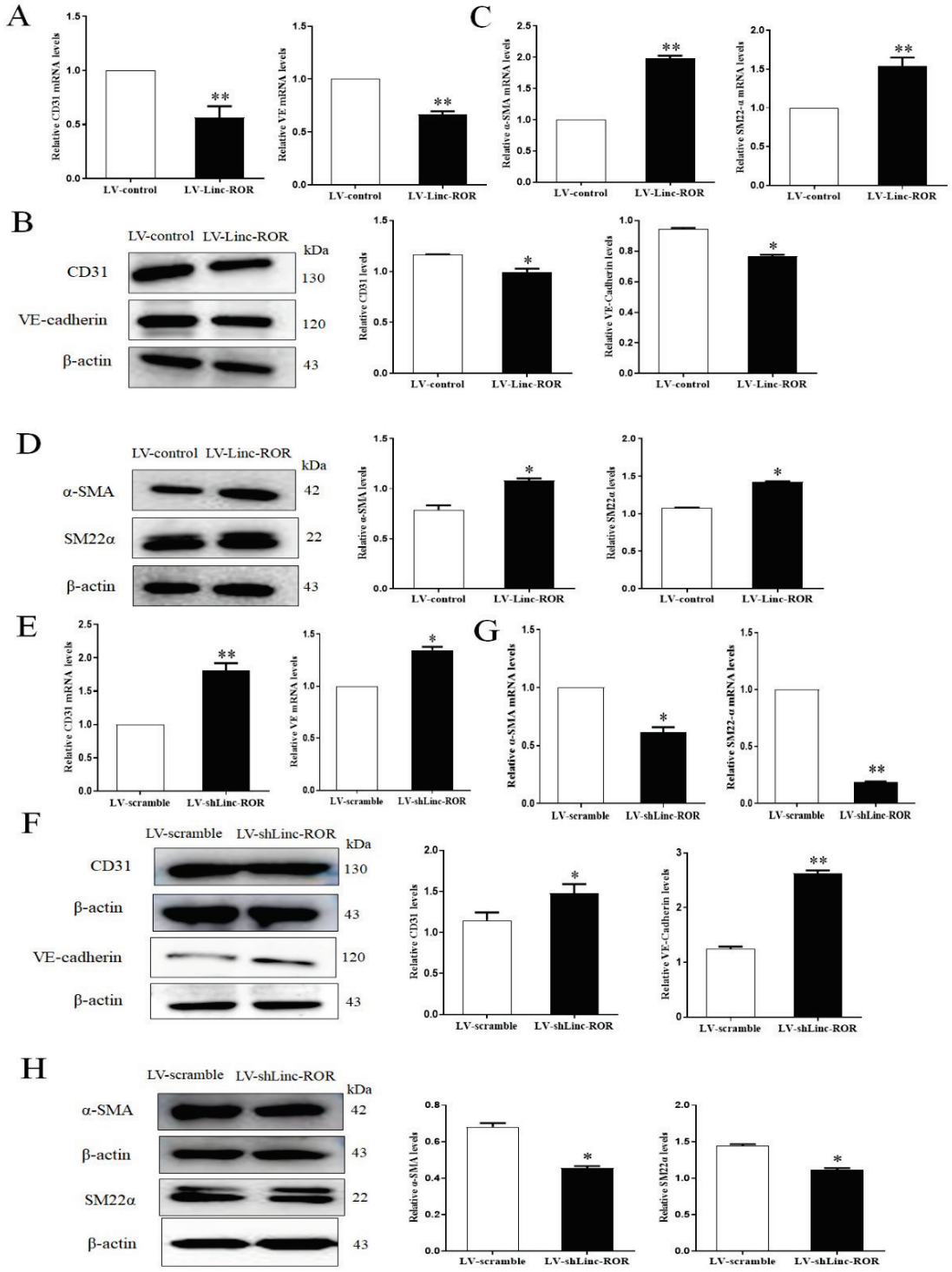

Fig. 4. Linc-ROR promoted EPC EndMT. (**A-D**) The qRT-PCR and WB assay showed that LV-linc-ROR downregulated the expression of the endothelial markers, CD31 and VE-cadherin, but upregulated the expression of the mesenchymal markers, SM22α and α-SMA, both at the mRNA and protein levels. (**E-H**) To the contrary, LV-shlinc-ROR obviously promoted the expression of CD31 and VE-cadherin, but inhibited the expression of α-SMA and SM22α both at the mRNA and protein levels. n=3, **P*<0.05, ***P*<0.01 *vs.* the LV-control or LV-scramble group.

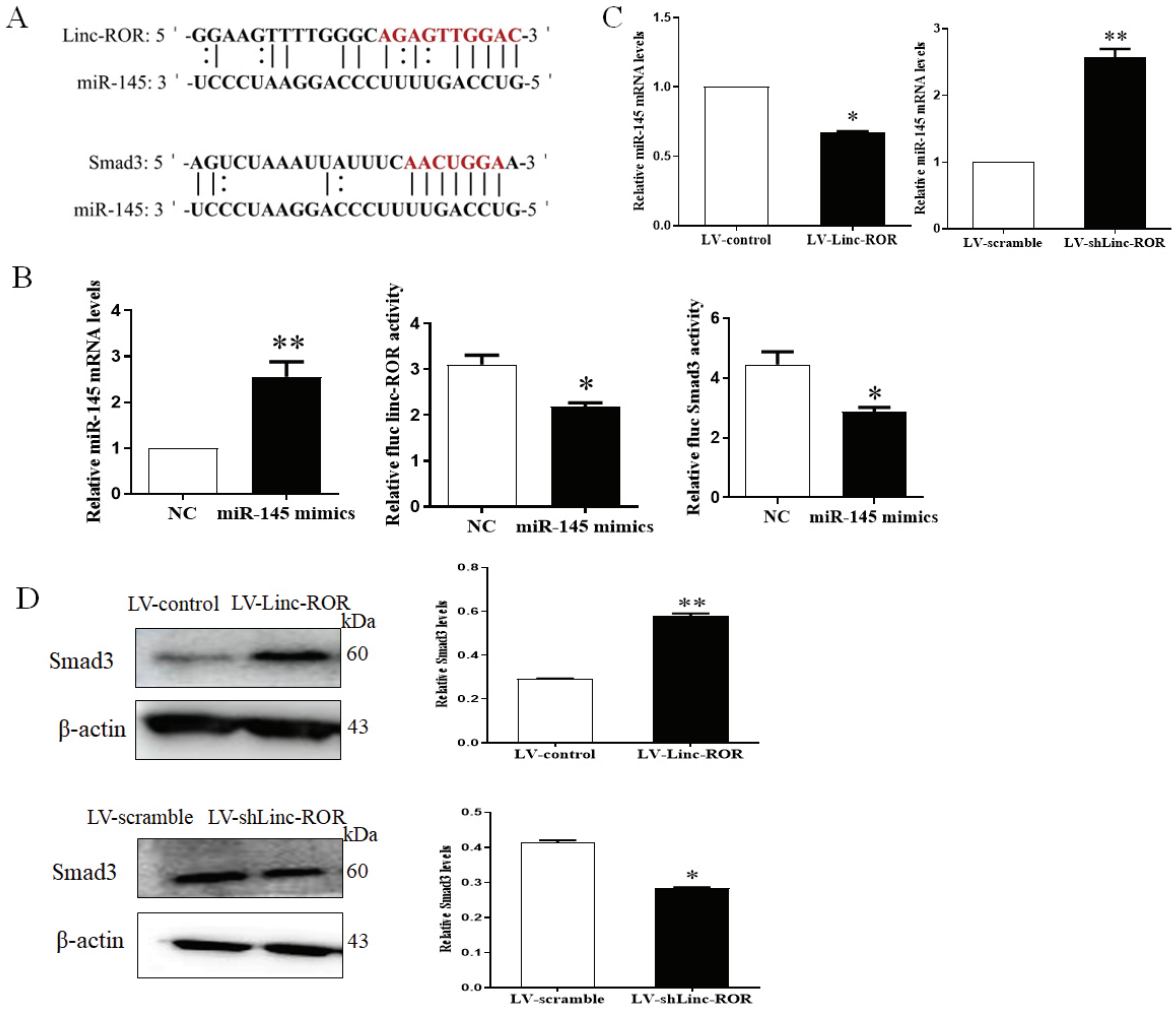

Fig. 5. Linc-ROR-miR-145-Smad3 signal pathway was involved in EPC EndMT. (**A**) The predicted binding sites between miR-145 with linc-ROR or Smad3 based on the TargetScan and miRanda databases. (**B**) MiR-145 mimics could increase the miR-145 level in 293T cells compared with the NC group. The dual luciferase reporter assay showed that linc-ROR bound to miR-145 and miR-145 bound to the 3'UTR of Smad3 mRNA. (**C**) LV-linc-ROR decreased the expression of miR-145, but LV-shlinc-ROR increased the expression of miR-145. (**D**) LV-linc-ROR increased the expression of Smad3, but LV-shlinc-ROR decreased the expression of Smad3 at the protein levels. n=3, **P*<0.05, ***P*<0.01 *vs.* the LV-control or LV-scramble group.

Previous evidence revealed that numerous miRNAs mediate the process of EndMT [32]. For example, miR-29a-5p mediated parathyroid hormone-induced-EndMT by targeting GASP [33]. In addition, the downregulation of miR-195-5p inhibited EndMT and myocardial fibrosis of diabetic cardiomyopathy by targeting Smad7 [34]. In EPCs, miR-126 could inhibit EndMT via the PIK3R2-PI3K/Akt signaling pathway [35]. Increasing evidence has shown that miR-145 acted as a tumor suppressor in a variety of cancer cells. Lei *et al* [36] pointed out that lincRNA-TUG1 contributed to the progression of thyroid cancer cells by sponging miR-145. Additionally, it has been shown that miR-145 could attenuate TGF-β-mediated EMT in non-small cell lung cancer [37].

The TGF-β pathway is one of the most important signal transduction pathways in EndMT. During the TGF-β mediated EndMT process, the Smad family of transcription factors is a central mediator of the TGF-β signaling pathway [38]. TGF-β subunits bind to either TGF-β type I or type II receptor, leading to the activation of Smad2 and 3, which interact with Smad4 to form a heterogeneous Smad complex which is translocated into the nucleus to activate corresponding gene expression [39,40]. Therefore, inhibiting the Smad family of transcription factors to hamper the activation of the TGF-β signaling pathway may block EndMT. Cooley *et al* [41] reported that abrogation of TGF-β signaling by short hairpin RNA-mediated Smad3 and haplo-insufficiency, resulting in decreased EndMT and reduced

neointimal formation. Therefore, the TGF-β/Smad3 signaling pathway was considered a potential target to inhibit EndMT. It has been shown that miR-145 could bind to the 3'-UTR of Smad3, thereby attenuating TGF-β/Smad3-mediated EMT in non-small cell lung cancer [37]. The current study verified that miR-145 binds to the 3'-UTR of Smad3, which indicated that miR-145 was involved in the EndMT process of EPCs. Moreover, western blotting revealed that linc-ROR promoted the protein expression of Smad3, while LV-shlinc-ROR inhibited the protein expression of Smad3.

Collectively, the findings of the current study demonstrated that linc-ROR promoted EPC EndMT as a competing endogenous RNA to regulate downstream Smad3 expression. The linc-ROR/miR-145/Smad3 axis should be considered in the study of the pathophysiology of cardiovascular diseases. The present study showed that inhibition of EPC EndMT by targeting the linc-ROR/miR-145/Smad3 signaling pathway could potentially be used as a novel therapeutic approach. Whereas, other unique characteristics of linc-ROR's effects on EndMT of EPCs should be considered in future studies.

Conflict of Interest

There is no conflict of interest.

Acknowledgements

This work was supported by the National Natural Science Foundation of China (81870237), Weifang Science and Technology Development Project (2023GX027) and College Student Innovation Training Program (S202310438210, X2023407).

References

1. Kovacic JC, Dimmeler S, Harvey RP, Finkel T, Aikawa E, Krenning G, Baker AH. Endothelial to mesenchymal transition in cardiovascular disease: JACC state-of-the-art review. J Am Coll Cardiol 2019;73:190-209. https://doi.org/10.1016/j.jacc.2018.09.089
2. Zhao X, Huang L, Yin Y, Fang Y, Zhou Y. Autologous endothelial progenitor cells transplantation promoting endothelial recovery in mice. Transpl Int 2007; 20:712-721. https://doi.org/10.1111/j.1432-2277.2007.00497.x
3. Toya SP, Malik AB. Role of endothelial injury in disease mechanisms and contribution of progenitor cells in mediating endothelial repair. Immunobiology 2012; 217: 569-580. https://doi.org/10.1016/j.imbio.2011.03.006
4. Diez M, Musri MM, Ferrer E, Barbera JA, Peinado VI. Endothelial progenitor cells undergo an endothelial-to-mesenchymal transition-like process mediated by TGFbetaRI. Cardiovasc Res 2010;88:502-511. https://doi.org/10.1093/cvr/cvq236
5. Moonen JR, Krenning G, Brinker MG, Koerts JA, van Luyn MJ, Harmsen MC. Endothelial progenitor cells give rise to pro-angiogenic smooth muscle-like progeny. Cardiovasc Res 2010; 86: 506-515. https://doi.org/10.1093/cvr/cvq012
6. Gao Y, Cui X, Wang M, Zhang Y, He Y, Li L, Li H, et al. Oscillatory shear stress induces the transition of EPCs into mesenchymal cells through ROS/PKCζ/p53 pathway. Life Sci 2020;253:117728. https://doi.org/10.1016/j.lfs.2020.117728
7. Alvarez-Dominguez JR, Hu W, Yuan B, Shi J, Park SS, Gromatzky AA, van Oudenaarden A, et al. Global discovery of erythroid long noncoding RNAs reveals novel regulators of red cell maturation. Blood 2014;123:570-581. https://doi.org/10.1182/blood-2013-10-530683
8. Mercer TR, Dinger ME, Mattick JS. Long non-coding RNAs: insights into functions. Nat Rev Genet 2009;10:155-159. https://doi.org/10.1038/nrg2521
9. Loewer S, Cabili MN, Guttman M, Loh YH, Thomas K, Park IH, Garber M, et al. Large intergenic non-coding RNA-ROR modulates reprogramming of human induced pluripotent stem cells. Nat Genet 2010;42:1113-1117. https://doi.org/10.1038/ng.710
10. Yi M, Wang S, Zhang X, Jiang L, Xia X, Zhang T, Fang X. Linc-ROR promotes EMT by targeting miR-204-5p/SMAD4 in endometriosis. Reprod Sci 2023;30:2665-2679. https://doi.org/10.1007/s43032-023-01204-0
11. Wen X, Wu Y, Lou Y, Xia Y, Yu X. The roles of Linc-ROR in the regulation of cancer stem cells. Transl Oncol 2023; 28:101602. https://doi.org/10.1016/j.tranon.2022.101602

12. Pan, Y, Chen, J, Tao, L, Zhang, K, Wang, R, Chu, X and Chen, L. Long noncoding RNA ROR regulates chemoresistance in docetaxel-resistant lung adenocarcinoma cells via epithelial mesenchymal transition pathway. Oncotarget 2017;8:33144-33158. https://doi.org/10.18632/oncotarget.16562
13. Wesseling M, Sakkers TR, De Jager S, Pasterkamp G and Goumans MJ. The morphological and molecular mechanisms of epithelial/endothelial-to-mesenchymal transition and its involvement in atherosclerosis. Vasc Pharmacol 2018;106:1-8. https://doi.org/10.1016/j.vph.2018.02.006
14. Qiu P, Feng XH and Li L. Interaction of Smad3 and SRF-associated complex mediates TGF-beta1 signals to regulate SM22 transcription during myofibroblast differentiation. J Mol Cell Cardiol 2003;35:1407-1420. https://doi.org/10.1016/j.yjmcc.2003.09.002
15. Cho HJ and Yoo J. Rho activation is required for transforming growth factor-beta-induced epithelial-mesenchymal transition in lens epithelial cells. Cell Biol Int 2007; 31:1225-1230. https://doi.org/10.1016/j.cellbi.2007.04.006
16. Li J, Qu X, Yao J, Caruana G, Ricardo S. D, Yamamoto Y, Yamamoto H, et al. Blockade of endothelial-mesenchymal transition by a Smad3 inhibitor delays the early development of streptozotocin-induced diabetic nephropathy. Diabetes 2010; 59:2612-2624. https://doi.org/10.2337/db09-1631
17. Gong F, Zhao F and Gan XD. Celastrol protects TGF-beta1-induced endothelial-mesenchymal transition. J Huazhong Univ Sci Technolog Med Sci 2017; 37:185-190. https://doi.org/10.1007/s11596-017-1713-0
18. Li L, Wen J, Li H, He Y, Cui X, Zhang X, Guan X, et al. Exosomal circ-1199 derived from EPCs exposed to oscillating shear stress acts as a sponge of let-7g-5p to promote endothelial-mesenchymal transition of EPCs by increasing HMGA2 expression. Life Sci 2023;312:121223. https://doi.org/10.1016/j.lfs.2022.121223
19. Hur J, Yoon C. H, Kim H. S, Choi J. H, Kang H. J, Hwang K. K, Oh B. H, et al. Characterization of two types of endothelial progenitor cells and their different contributions to neovasculogenesis. Arterioscler Thromb Vasc Biol 2004;24:288-293. https://doi.org/10.1161/01.ATV.0000114236.77009.06
20. Sieveking D. P, Buckle A, Celermajer D. S and Ng M. K. Strikingly different angiogenic properties of endothelial progenitor cell subpopulations: insights from a novel human angiogenesis assay. J Am Coll Cardiol 2008;51:660-668. https://doi.org/10.1016/j.jacc.2007.09.059
21. Rostam-Alilou AA, Jarrah HR, Zolfagharian A and Bodaghi M. Fluid-structure interaction (FSI) simulation for studying the impact of atherosclerosis on hemodynamics, arterial tissue remodeling, and initiation risk of intracranial aneurysms. Biomech Model Mechan 2022;21:1393-1406. https://doi.org/10.1007/s10237-022-01597-y
22. Alvandi Z, Nagata Y, Passos L, Hashemi G. A, Guerrero J. L, Wylie-Sears J, Romero D. C, et al. Wnt site signaling inhibitor secreted frizzled-related protein 3 protects mitral valve endothelium from myocardial infarction-induced endothelial-to-mesenchymal transition. J Am Heart Assoc 2022;11:e23695. https://doi.org/10.1161/JAHA.121.023695
23. Sabbineni H, Verma A, Artham S, Anderson D, Amaka O, Liu F, Narayanan SP, et al. Pharmacological inhibition of beta-catenin prevents EndMT in vitro and vascular remodeling in vivo resulting from endothelial Akt1 suppression. Biochem Pharmacol 2019; 164: 205-215. https://doi.org/10.1016/j.bcp.2019.04.016
24. Hashimoto N, Phan SH, Imaizumi K, Matsuo M, Nakashima H, Kawabe T, Shimokata K, et al. Endothelial-mesenchymal transition in bleomycin-induced pulmonary fibrosis. Am J Resp Cell Mol 2010; 43: 161-172. https://doi.org/10.1165/rcmb.2009-0031OC
25. Ma K, Li C, Xu J, Ren F, Xu X, Liu C, Niu B, et al. LncRNA Gm16410 regulates PM2.5-induced lung endothelial-mesenchymal transition via the TGF-β1/Smad3/p-Smad3 pathway. Ecotoxicol Environ Saf 2020;205:111327. https://doi.org/10.1016/j.ecoenv.2020.111327
26. Yin Q, He M, Huang L, Zhang X, Zhan J, Hu J. LncRNA ZFAS1 promotes ox-LDL induced EndMT through miR-150-5p/Notch3 signaling axis. Microvasc Res 2021;134:104118. https://doi.org/10.1016/j.mvr.2020.104118
27. Zhang R, Huang XQ, Jiang YY, Li N, Wang J, Chen SY. LncRNA TUG1 regulates autophagy-mediated endothelial-mesenchymal transition of liver sinusoidal endothelial cells by sponging miR-142-3p. Am J Transl Res 2020;12:758-772.
28. Ghafouri-Fard S, Pourtavakoli A, Hussen BM, Taheri M and Kiani A. A review on the importance of LINC-ROR in human disorders. Pathol Res Pract 2023;244:154420. https://doi.org/10.1016/j.prp.2023.154420

29. Ma X, Zhang H, Li Q, Schiferle E, Qin Y, Xiao S, Li T. FOXM1 promotes head and neck squamous cell carcinoma via activation of the Linc-ROR /LMO4/AKT/PI3K axis. Front Oncol 2021;11:658712. https://doi.org/10.3389/fonc.2021.658712
30. Li J, Zhang S, Wu L, Pei M. Interaction between LncRNA-ROR and miR-145 contributes to epithelial-mesenchymal transition of ovarian cancer cells. Gen Physiol Biophys 2019;38:461-471. https://doi.org/10.4149/gpb_2019028
31. Ge H, Liu J, Liu F, Sun Y and Yang R. Long non-coding RNA ROR mitigates cobalt chloride-induced hypoxia injury through regulation of miR-145. Artif Cell Nanomed Bio 2019;47:2221-2229. https://doi.org/10.1080/21691401.2019.1620759
32. Hulshoff MS, Del MG, Kovacic J, Krenning G. Non-coding RNA in endothelial-to-mesenchymal transition. Cardiovasc Res 2019;115:1716-1731. https://doi.org/10.1093/cvr/cvz211
33. Wang L, Tang R, Zhang Y, Chen S, Guo Y, Wang X, Liu Z, et al. PTH-induced EndMT via miR-29a-5p/GSAP/Notch1 pathway contributed to valvular calcification in rats with CKD. Cell Prolif 2021;54:e13018. https://doi.org/10.1111/cpr.13018
34. Ding H, Yao J, Xie H, Wang C, Chen J, Wei K, Ji Y, et al. MicroRNA-195-5p downregulation inhibits endothelial mesenchymal transition and myocardial fibrosis in diabetic cardiomyopathy by targeting smad7 and inhibiting transforming growth factor beta1-smads-snail pathway. Front Physiol 2021;12:709123. https://doi.org/10.3389/fphys.2021.709123
35. Zhang J, Zhang Z, Zhang DY, Zhu J, Zhang T, Wang C. MicroRNA 126 inhibits the transition of endothelial progenitor cells to mesenchymal cells via the PIK3R2-PI3K/AKT signalling pathway. PLoS One 2013;8:e83294. https://doi.org/10.1371/journal.pone.0083294
36. Lei H, Gao Y, Xu X. LncRNA TUG1 influences papillary thyroid cancer cell proliferation, migration and EMT formation through targeting miR-145. Acta Biochim Biophys Sin 2017;49:588-597. https://doi.org/10.1093/abbs/gmx047
37. Hu H, Xu Z, Li C, Xu C, Lei Z, Zhang HT, Zhao J. Mir-145 and miR-203 represses TGF-β-induced epithelial-mesenchymal transition and invasion by inhibiting SMAD3 in non-small cell lung cancer cells. Lung Cancer 2016;97:87-94. https://doi.org/10.1016/j.lungcan.2016.04.017
38. Tian J, Zhang M, Suo M, Liu D, Wang X, Liu M, Pan J, et al. Dapagliflozin alleviates cardiac fibrosis through suppressing EndMT and fibroblast activation via AMPKα/ TGF-β/Smad signalling in type 2 diabetic rats. J Cell Mol Med 2021;25:7642-7659. https://doi.org/10.1111/jcmm.16601
39. Roberts AB, Tian F, Byfield SD, Stuelten C, Ooshima A, Saika S, Flanders KC. Smad3 is key to TGF-beta-mediated epithelial-to-mesenchymal transition, fibrosis, tumor suppression and metastasis. Cytokine Growth Factor Rev 2006;17:19-27. https://doi.org/10.1016/j.cytogfr.2005.09.008
40. Song S, Zhang R, Cao W, Fang G, Yu Y, Wan Y, Wang C, et al. Foxm1 is a critical driver of TGF-β-induced EndMT in endothelial cells through Smad2/3 and binds to the snail promoter. J Cell Physiol 2019;234:9052-9064. https://doi.org/10.1002/jcp.27583
41. Cooley BC, Nevado J, Mellad J, Yang D, St HC, Negro A, Fang F, et al. TGF-β signaling mediates endothelial-to-mesenchymal transition (EndMT) during vein graft remodeling. Sci Transl Med 2014;6:227-234. https://doi.org/10.1126/scitranslmed.3006927